Computational Mechanics 25 (2000) 376–384 © Springer-Verlag 2000

Development of eight-node quadrilateral membrane elements using the area coordinates method

Soh Ai-Kah, Long Yuqiu, Cen Song

Abstract Two eight-node quadrilateral elements, namely, AQ8-I and AQ8-II, have been developed using the quadrilateral area coordinate and generalized conforming methods. Some appropriate examples were employed to evaluate the performance of the proposed elements. The numerical results show that the proposed elements are superior to the standard eight-node isoparametric element, thereafter called Q8. This is because the former does not only possess the same accuracy as the latter when regular meshes are employed for analysis, but is also very insensitive to mesh distortion, for which the Q8 element can not handle. It has also been demonstrated that the area coordinate method is an efficient tool for developing simple, effective and reliable serendipity plane membrane elements.

1 Introduction

It has been a common practice to construct quadrilateral elements using isoparametric coordinates (ξ, η). However, such formulation approach has several well-known disadvantages: (1) The element local coordinates (ξ, η) are irrational functions of the Cartesian coordinates (x, y) and, therefore, the former can not be expressed in terms of the latter in finite terms except for the degenerate case of a parallelogram. (2) The element stiffness matrix contains the determinant of Jacobian inverse, for which the value obtained by numerical integration is usually only an approximation in most of the ordinary cases.

The area coordinate method has been widely used to construct triangular elements. Long et al. [1] has generalized the said method to construct quadrilateral elements. The quadrilateral area coordinates are natural and linearly related to Cartesian coordinates. Furthermore, there is no necessity to perform numerical integration for those formulae expressed in terms of area coordinates, and the exact results can be obtained if numerical integration is carried out. Thus, the area coordinate method provides a new tool for developing quadrilateral elements. Some basic formulae, established using the area coordinate system, for the development of quadrilateral elements have been presented by Long et al. [2].

The 8-node isoparametric element (Q8) is one of the most commonly used elements and its performance has been thoroughly assessed by researchers. Stricklin et al. [3] presented some results for a cantilever beam modeled using distorted and undistorted elements, and they showed that the 8-node isoparametric element stiffened and performed very badly when it was distorted. Lee [4] studied the various influences to some serendipity (Q8, Q12) and Lagrangian (Q9, Q16) elements using various distorted meshes. He pointed out that the displacement fields of Q8 and Q12 are only C_1 completeness under distorted conditions, while Q9 and Q16 could reach much higher order of completeness. Therefore, the Lagrangian element types embody better stability in most cases, and were strongly recommended by Lee. Zienkiewicz [5] has made the same conclusion. Unfortunately, all Lagrangian elements possess internal nodes and their formulations are more complicated than those of the corresponding serendipity elements. Thus, the latter is still preferred in practical applications.

The objectives of this paper are two folds: (1) to construct quadrilateral elements by employing the quadrilateral area coordinates; and (2) to examine the potential accuracy and versatility of the new tool. The concept of generalized conforming [6, 7] will also be applied in the element formulations. This is to say there is no necessity to implement exact compatibility between two elements, and only some relaxed compatibility conditions are imposed. The said relaxed requirement provides more freedom for selecting interpolation functions for the displacement fields within the element. Moreover, it assures the convergence of results [8, 9]. For example, the displacement fields could be assumed to satisfy the following conditions:

$$\begin{cases} (u-\tilde{u})_j = 0 \\ (v-\tilde{v})_j = 0 \end{cases} \quad \text{(at each node } j\text{)} \tag{1}$$

$$\begin{cases} \int_{d_i}(u-\tilde{u})\mathrm{d}s = 0 \\ \int_{d_i}(v-\tilde{v})\mathrm{d}s = 0 \end{cases} \quad \text{(along each side } d_i\text{)} \tag{2}$$

where (u, v) are the displacement fields within one element, and $(\tilde{u}, \tilde{v})$ are the displacements on the boundary of the element. Note that Eq. (1) is the point compatibility condition for nodal deflection at each node, and Eq. (2) is

Received 11 August 1999

Soh Ai-Kah (✉)
Department of Mechanical Engineering,
The University of Hong Kong, Hong Kong

Long Yuqiu, Cen Song
Department of Civil Engineering, Tsinghua University,
100084, Beijing, China

The work described in this paper was supported by grants from the Research Grants Council of the Hong Kong Special Administrative Region, China (Project No. HKU7122/99E), and the Natural Science Foundation of China (59878022).

the line compatibility conditions for the average deflection along each side of the element. This step would soften the elements.

In this paper, two 8-node quadrilateral membrane elements, AQ8-I and AQ8-II, will be developed using the area coordinates and generalized conforming method. Some appropriate examples will be employed to evaluate the performance of the proposed elements.

2
Area coordinates for quadrilateral elements

Consider an 8-node straight-side serendipity element, as shown in Fig. 1. Nodes 1, 2, 3 and 4 are the corner nodes; and nodes 5, 6, 7 and 8 are the mid-side nodes of sides $\overline{12}, \overline{23}, \overline{34}$ and $\overline{41}$, respectively. The position of an arbitrary point P within the element is specified by the area coordinates L_1, L_2, L_3 and L_4, which are defined as

$$L_i = \frac{A_i}{A} \quad (i = 1, 2, 3, 4) \tag{3}$$

where A is the area of the quadrilateral element, A_i is the area of the triangle constructed by point P and the ith side of the element.

L_1, L_2, L_3 and L_4 can be expressed in terms of Cartesian coordinates (x, y) as follows:

$$L_i = \frac{1}{2A}(a_i + b_i x + c_i y) \quad (i = 1, 2, 3, 4) \tag{4}$$

where

$$\begin{aligned} &a_i = x_j y_k - x_k y_j, \quad b_i = y_j - y_k, \\ &c_i = x_k - x_j \quad (\overleftarrow{i, j, k} = \overleftarrow{1, 2, 3, 4}) \end{aligned} \tag{5}$$

and (x_i, y_i) $(i = 1, 2, 3, 4)$ are the Cartesian coordinates of the four corner nodes.

Introduce four dimensionless parameters g_1, g_2, g_3 and g_4 to each of the quadrangles, as shown in Fig. 2. These parameters are defined as

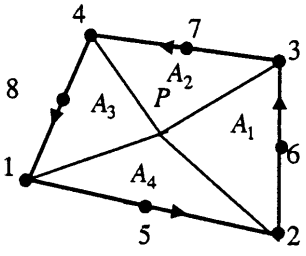

Fig. 1. Definition of area coordinates L_i

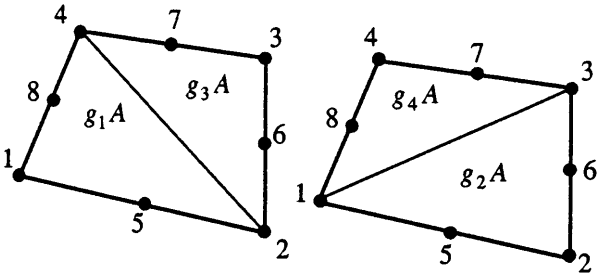

Fig. 2. Definition of four parameters g_1, g_2, g_3 and g_4

$$g_1 = \frac{A'}{A}, \quad g_2 = \frac{A''}{A}, \quad g_3 = 1 - g_1, \quad g_4 = 1 - g_2 \tag{6}$$

where A' and A'' are the areas of $\Delta 124$ and $\Delta 123$, respectively.

It is obvious that any point in a plane problem has two degrees of freedom. Therefore, only two of the coordinates L_i $(i = 1, 2, 3, 4)$ are independent. It can be shown that L_i $(i = 1, 2, 3, 4)$ must satisfy [1] the following conditions:

$$L_1 + L_2 + L_3 + L_4 = 1 \tag{7}$$

$$g_4 g_1 L_1 - g_1 g_2 L_2 + g_2 g_3 L_3 - g_3 g_4 L_4 = 0 \tag{8}$$

Note that L_i $(i = 1, 2, 3, 4)$ can also be expressed in terms of the quadrilateral isoparametric coordinates (ξ, η) as follows:

$$\begin{aligned} L_1 &= \tfrac{1}{4}(1 - \xi)[g_2(1 - \eta) + g_3(1 + \eta)] \\ L_2 &= \tfrac{1}{4}(1 - \eta)[g_4(1 - \xi) + g_3(1 + \xi)] \\ L_3 &= \tfrac{1}{4}(1 + \xi)[g_1(1 - \eta) + g_4(1 + \eta)] \\ L_4 &= \tfrac{1}{4}(1 + \eta)[g_1(1 - \xi) + g_2(1 + \xi)] \end{aligned} \tag{9}$$

The coordinates of the eight nodes are:

node 1: $(g_2, g_4, 0, 0)$ node 5: $\left(\frac{g_2}{2}, \frac{g_3 + g_4}{2}, \frac{g_1}{2}, 0\right)$

node 2: $(0, g_3, g_1, 0)$ node 6: $\left(0, \frac{g_3}{2}, \frac{g_4 + g_1}{2}, \frac{g_2}{2}\right)$

node 3: $(0, 0, g_4, g_2)$ node 7: $\left(\frac{g_3}{2}, 0, \frac{g_4}{2}, \frac{g_1 + g_2}{2}\right)$

node 4: $(g_3, 0, 0, g_1)$ node 8: $\left(\frac{g_2 + g_3}{2}, \frac{g_4}{2}, 0, \frac{g_1}{2}\right)$

In a quadrilateral element, the following basic formulae can be used to evaluate the line integral for arbitrary power functions of area coordinates along each side $L_i = 0$ $(i = 1, 2, 3, 4)$:

(i) Along side $\overline{12}$ $(L_4 = 0)$:

$$\int_0^1 L_1^m L_2^n L_3^p \, \mathrm{d}\bar{s} = \frac{m! n! p!}{(m + n + p + 1)!} g_2^m g_1^p \sum_{k=0}^{n} g_3^{n-k} g_4^k C_{p+n-k}^p C_{m+k}^m \tag{10}$$

(ii) Along side $\overline{23}$ $(L_1 = 0)$:

$$\int_0^1 L_2^n L_3^p L_4^q \, \mathrm{d}\bar{s} = \frac{n! p! q!}{(n + p + q + 1)!} g_3^n g_2^q \sum_{k=0}^{p} g_4^{p-k} g_1^k C_{q+p-k}^q C_{n+k}^n \tag{11}$$

(iii) Along side $\overline{34}$ $(L_2 = 0)$:

$$\int_0^1 L_3^p L_4^q L_1^m \, \mathrm{d}\bar{s} = \frac{p! q! m!}{(p + q + m + 1)!} g_4^p g_3^m \sum_{k=0}^{q} g_1^{q-k} g_2^k C_{m+q-k}^m C_{p+k}^p \tag{12}$$

(iv) Along side $\overline{41}$ ($L_3 = 0$):

$$\int_0^1 L_4^q L_1^m L_2^n \, \mathrm{d}\bar{s} = \frac{q!m!n!}{(q+m+n+1)!} g_1^q g_4^n \sum_{k=0}^{m} g_2^{m-k} g_3^k C_{n+m-k}^n C_{q+k}^q \tag{13}$$

where $\bar{s}$ is a dimensionless coordinate along each side, and it is 0 at the starting node and 1 at ending node; m, n, p, and q are arbitrary positive integers; and C_m^n is defined as

$$C_m^n = \frac{m!}{(m-n)!n!} \quad (m > n) \tag{14}$$

3 Shape functions of the new 8-node quadrilateral elements

3.1 Preparatory shape functions for corner nodes

Firstly, prescribe a set of "shape functions" for the four corner nodes:

$$\begin{cases} N_1^0 = \dfrac{L_1}{2g_2}\left(1 - \dfrac{L_4}{g_1}\right) + \dfrac{L_2}{2g_4}\left(1 - \dfrac{L_3}{g_1}\right) \\ N_2^0 = \dfrac{L_2}{2g_3}\left(1 - \dfrac{L_1}{g_2}\right) + \dfrac{L_3}{2g_1}\left(1 - \dfrac{L_4}{g_2}\right) \\ N_3^0 = \dfrac{L_3}{2g_4}\left(1 - \dfrac{L_2}{g_3}\right) + \dfrac{L_4}{2g_2}\left(1 - \dfrac{L_1}{g_3}\right) \\ N_4^0 = \dfrac{L_4}{2g_1}\left(1 - \dfrac{L_3}{g_4}\right) + \dfrac{L_1}{2g_3}\left(1 - \dfrac{L_2}{g_4}\right) \end{cases} \tag{15}$$

i.e.

$$N_i^0 = \frac{L_i}{2g_j}\left(1 - \frac{L_m}{g_i}\right) + \frac{L_j}{2g_m}\left(1 - \frac{L_k}{g_i}\right) \quad (\overleftrightarrow{i,j,k,m} = \overleftrightarrow{1,2,3,4}) \tag{16}$$

It can be clearly seen that N_i^0 ($i = 1, 2, 3, 4$), which are quadratic, satisfy the following conditions:

$$N_i^0((L_1)_j, (L_2)_j, (L_3)_j, (L_4)_j) = \delta_{ij} = \begin{cases} 1 & (i = j) \\ 0 & (i \neq j) \end{cases} \quad (i, j = 1, 2, 3, 4) \tag{17}$$

But N_i^0 are not zero at mid-side nodes 5, 6, 7 and 8. Thus, they cannot be the real shape functions for the corner nodes. Therefore, they are called the preparatory shape functions for corner nodes.

3.2 Shape functions for mid-side nodes

Secondly, define two sets of shape functions for the mid-side nodes as follows:

(i)

$$\begin{aligned} N_5 &= \frac{2}{g_1 g_2} L_1 L_3 \left(1 + \frac{2}{g_3 + g_4} L_2 - \frac{2}{g_1 + g_2} L_4\right) \\ N_6 &= \frac{2}{g_2 g_3} L_2 L_4 \left(1 + \frac{2}{g_4 + g_1} L_3 - \frac{2}{g_2 + g_3} L_1\right) \\ N_7 &= \frac{2}{g_3 g_4} L_3 L_1 \left(1 + \frac{2}{g_1 + g_2} L_4 - \frac{2}{g_3 + g_4} L_2\right) \\ N_8 &= \frac{2}{g_4 g_1} L_4 L_2 \left(1 + \frac{2}{g_2 + g_3} L_1 - \frac{2}{g_4 + g_1} L_3\right) \end{aligned} \tag{18}$$

i.e.

$$N_{4+i} = \frac{2}{g_i g_j} L_i L_k \left(1 + \frac{2}{g_k + g_m} L_j - \frac{2}{g_i + g_j} L_m\right) \quad (\overleftrightarrow{i,j,k,m} = \overleftrightarrow{1,2,3,4}) \tag{19}$$

(ii)

$$\begin{aligned} N_5 &= \frac{4}{g_1 g_2} L_1 L_3 \left(L_2 - L_4 + \frac{g_1 + g_2}{2}\right) \\ N_6 &= \frac{4}{g_2 g_3} L_2 L_4 \left(L_3 - L_1 + \frac{g_2 + g_3}{2}\right) \\ N_7 &= \frac{4}{g_3 g_4} L_3 L_1 \left(L_4 - L_2 + \frac{g_3 + g_4}{2}\right) \\ N_8 &= \frac{4}{g_4 g_1} L_4 L_2 \left(L_1 - L_3 + \frac{g_4 + g_1}{2}\right) \end{aligned} \tag{20}$$

i.e.

$$N_{4+i} = \frac{4}{g_i g_j} L_i L_k \left(L_j - L_m + \frac{g_i + g_j}{2}\right) \quad (\overleftrightarrow{i,j,k,m} = \overleftrightarrow{1,2,3,4}) \tag{21}$$

It can be clearly seen that both sets of N_i ($i = 5, 6, 7, 8$) satisfy:

$$N_i((L_1)_j, (L_2)_j, (L_3)_j, (L_4)_j) = \delta_{ij} = \begin{cases} 1 & (i = j) \\ 0 & (i \neq j) \end{cases} \quad (i = 5, 6, 7, 8,\ j = 1, 2, \ldots, 7, 8) \tag{22}$$

Let Z_i ($i = 1, 2, 3, 4$) be the difference between the shape functions given by Eqs. (19) and (21). Thus, we obtain

$$Z_i = (N_{4+i})^{\mathrm{I}} - (N_{4+i})^{\mathrm{II}} = \frac{1 - g_i - g_j}{g_i g_j} L_i L_k \left[\frac{1}{2} - \left(\frac{L_j}{g_k + g_m} + \frac{L_m}{g_i + g_j}\right)\right] \quad (\overleftrightarrow{i,j,k,m} = \overleftrightarrow{1,2,3,4}) \tag{23}$$

Substituting the equations of each element side, $L_i = 0$ ($i = 1, 2, 3, 4$), and the coordinates of the nodal points on each side into Eq. (23), we find that Z_i is always zero along the element sides. This is to say, Eqs. (19) and (21) are the same along the element sides. But within the element, the bubble function Z_i ($i = 1, 2, 3, 4$) for these two elements are different.

3.3
Shape functions for corner nodes

For corner nodes, the following modified shape functions are employed:

$$N_i = N_i^0 - \left(\frac{1}{2} - \frac{g_i - g_j}{8g_m}\right)N_{4+i} - \frac{g_k(g_j - g_k)}{8g_m g_i}N_{4+j} + \frac{g_k(g_k - g_m)}{8g_i g_j}N_{4+k} - \left(\frac{1}{2} + \frac{g_m - g_i}{8g_j}\right)N_{4+m} \quad (\overleftrightarrow{i,j,k,m} = \overleftrightarrow{1,2,3,4}) \tag{24}$$

It is obvious that N_i $(i = 1, 2, 3, 4)$ satisfy:

$$N_i((L_1)_j, (L_2)_j, (L_3)_j, (L_4)_j) = \delta_{ij} = \begin{cases} 1 & (i = j) \\ 0 & (i \neq j) \end{cases} \quad (i = 1, 2, 3, 4,\ j = 1, 2, \ldots, 7, 8) \tag{25}$$

3.4
Shape functions for two new elements

Equations (24) and (19) constitute a set of shape functions for an 8-node quadrilateral element, which is denoted as AQ8-I.

Another set of shape functions can be obtained by combining Eqs. (24) and (21) for developing a different 8-node quadrilateral element denoted by AQ8-II.

Note that the shape functions of these two elements are all cubic, both within and along the sides $(L_i = 0,\ i = 1, 2, 3, 4)$ of the elements. The displacement fields composed by these two sets of shape functions satisfy both the point and the side average conforming conditions, refer to Eqs. (1) and (2), respectively. Therefore, the AQ8-I and AQ8-II elements are generalized conforming elements. Figure 3 displays the process of the construction. When the element degenerates to a rectangular element, the shape functions of AQ8-I and AQ8-II will be the same as those of the Q8 element.

4
The stiffness matrix and efficient load vector

4.1
Stiffness matrices of the new elements

The displacement field of the element is given by:

$$\begin{Bmatrix} u \\ v \end{Bmatrix} = [\mathbf{N}]\{\mathbf{q}\}^e \tag{26}$$

where

$$\{\mathbf{q}\}^e = [u_1\ v_1\ u_2\ v_2\ u_3\ v_3\ u_4\ v_4\ u_5\ v_5\ u_6\ v_6\ u_7\ v_7\ u_8\ v_8]^{\mathrm{T}} \tag{27}$$

$$[\mathbf{N}] = [\mathbf{N}_1\ \mathbf{N}_2\ \mathbf{N}_3\ \mathbf{N}_4\ \mathbf{N}_5\ \mathbf{N}_6\ \mathbf{N}_7\ \mathbf{N}_8] \tag{28}$$

$$[\mathbf{N}_i] = \begin{bmatrix} N_i & 0 \\ 0 & N_i \end{bmatrix} \quad (i = 1, 2, \ldots, 8) \tag{29}$$

The strain field of the element is given by:

$$\{\boldsymbol{\varepsilon}\} = [\mathbf{B}]\{\mathbf{q}\}^e \tag{30}$$

where

$$\{\boldsymbol{\varepsilon}\} = \{\varepsilon_x\ \varepsilon_y\ \gamma_{xy}\}^{\mathrm{T}} \tag{31}$$

$$[\mathbf{B}] = [\mathbf{B}_1\ \mathbf{B}_2\ \mathbf{B}_3\ \mathbf{B}_4\ \mathbf{B}_5\ \mathbf{B}_6\ \mathbf{B}_7\ \mathbf{B}_8] \tag{32}$$

$$[\mathbf{B}_i] = \begin{bmatrix} \frac{\partial N_i}{\partial x} & 0 \\ 0 & \frac{\partial N_i}{\partial y} \\ \frac{\partial N_i}{\partial y} & \frac{\partial N_i}{\partial x} \end{bmatrix} \quad (i = 1, 2, \ldots, 8) \tag{33}$$

and

$$\begin{Bmatrix} \frac{\partial}{\partial x} \\ \frac{\partial}{\partial y} \end{Bmatrix} = \frac{1}{2A}\begin{bmatrix} b_1 & b_2 & b_3 & b_4 \\ c_1 & c_2 & c_3 & c_4 \end{bmatrix}\begin{Bmatrix} \frac{\partial}{\partial L_1} \\ \frac{\partial}{\partial L_2} \\ \frac{\partial}{\partial L_3} \\ \frac{\partial}{\partial L_4} \end{Bmatrix} \tag{34}$$

The evaluation of $\partial N_i/\partial x$ and $\partial N_i/\partial y$ are presented in the Appendix.

The element stiffness matrix can then be expressed as:

$$[\mathbf{K}]^e = \iint_A [\mathbf{B}]^{\mathrm{T}}[\mathbf{D}][\mathbf{B}]t\,\mathrm{d}A \tag{35}$$

where $[\mathbf{D}]$ and t are the elasticity matrix and the thickness of the element, respectively. For plane stress problems, we have

$$[\mathbf{D}] = \frac{E}{1 - \mu^2}\begin{bmatrix} 1 & \mu & 0 \\ \mu & 1 & 0 \\ 0 & 0 & \frac{1-\mu}{2} \end{bmatrix} \tag{36}$$

where E and μ are Young's modulus and Poisson's ratio, respectively. For plane strain problems, the E and μ in Eq. (36) should be replaced by $E/(1 - \mu^2)$ and $\mu/(1 - \mu)$, respectively.

By using the integration formulae for area coordinates in quadrilateral elements [2], the explicit expression of $[\mathbf{K}]^e$ can be obtained for straight-side elements. However, the numerical integration method would be more convenient

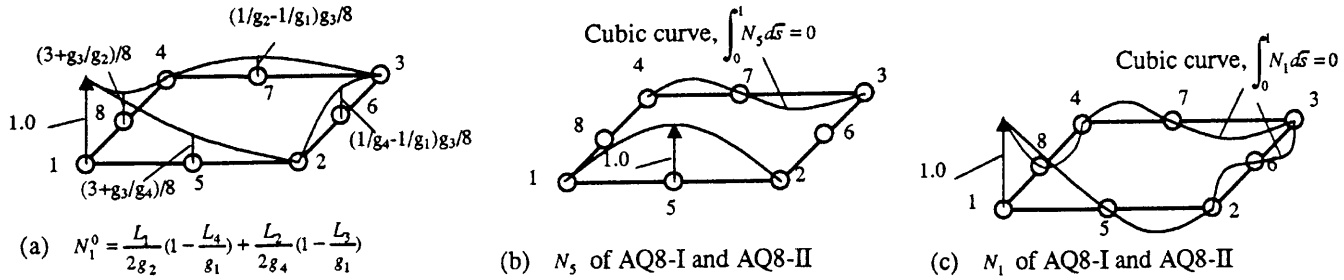

(a) $N_1^0 = \frac{L_1}{2g_2}(1 - \frac{L_4}{g_1}) + \frac{L_2}{2g_4}(1 - \frac{L_2}{g_1})$ (b) N_5 of AQ8-I and AQ8-II (c) N_1 of AQ8-I and AQ8-II

Fig. 3. Construction process of AQ8-I and AQ8-II

for computer coding. Thus, Eq. (35) is expressed in terms of isoparametric coordinates as follows:

$$[\mathbf{K}]^e = \int_{-1}^{1}\int_{-1}^{1} [\mathbf{B}]^{\mathrm{T}}[\mathbf{D}][\mathbf{B}]t|\mathbf{J}|\mathrm{d}\xi\,\mathrm{d}\eta \tag{37}$$

where $|\mathbf{J}|$ is the Jacobian determinant, which is the same as that of the 4-node isoparametric element. Since there are no $[\mathbf{J}]^{-1}$ (the Jacobian inverse) in $[\mathbf{B}]$, as long as the element sides are straight, exact value of $[\mathbf{K}]^e$ can be determined by numerical integration when the 3×3 Gauss integration points are employed. It is obvious that the results of Eq. (37) are only approximated values when the element sides are curved.

4.2
Efficient load vector for the new elements

The efficient load vector can be obtained using the standard approach. For the distributed load along the element side, the consistent element nodal load can be expressed as

$$\{\mathbf{R}\}^e_{16\times1} = \{R_{x1}\ R_{y1}\ R_{x2}\ R_{y2}\ R_{x3}\ \cdots\ R_{x8}\ R_{y8}\}^{\mathrm{T}} = \int_{\bar{s}} [\mathbf{N}]^{\mathrm{T}}\{\mathbf{f}\}_{2\times1}\,\mathrm{d}\bar{s} \tag{38}$$

where $\bar{s}$ denotes the direction along element side; and the distributed load vector $\{\mathbf{f}\}_{2\times1}$ is given by

$$\{\mathbf{f}\}_{2\times1} = [f_x\ f_y]^{\mathrm{T}} \tag{39}$$

where f_x and f_y are the distributed load functions in the x and y directions, respectively, along the element side.

5
Numerical examples

Example 1. *Patch test*. A small patch is discretized into some arbitrary elements, as shown in Fig. 4. The displacement fields corresponding to the constant strain are:

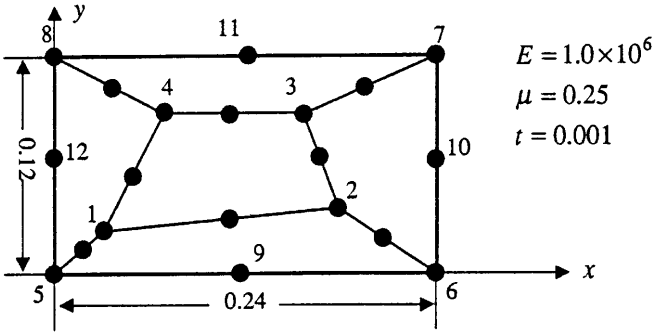

Fig. 4. Patch test

Table 1. Patch Test

Node	Coordinates		Displacement ($\times10^{-3}$)	
	x_i	y_i	u_i	v_i
1	0.04	0.02	0.05	0.04
2	0.18	0.03	0.195	0.12
3	0.16	0.08	0.20	0.16
4	0.18	0.08	0.12	0.12
5	0.00	0.00	0.00	0.00
6	0.24	0.00	0.24	0.12
7	0.24	0.12	0.30	0.24
8	0.00	0.12	0.06	0.12
9	0.12	0.00	0.12	0.06
10	0.24	0.06	0.27	0.18
11	0.12	0.12	0.18	0.18
12	0.00	0.06	0.03	0.06

$$u = 10^{-3}(x + y/2)$$
$$v = 10^{-3}(y + x/2)$$

The exact solution is as follows:

$$\sigma_x = \sigma_y = 1333.3333, \quad \tau_{xy} = 400.0$$

The coordinates and the displacement of control nodes are shown in Table 1.

The displacements of the boundary nodes (5–12), as shown in Table 1, are the displacement boundary conditions. The exact results of the displacements and stresses at each node can be obtained using the AQ8-I and AQ8-II elements. This demonstrates that the new elements pass the patch test and are able to ensure convergence.

Example 2. *Constant-bending-moment problem for a cantilever beam* (refer to Fig. 5). The results of the deflections and stresses at selected points are shown in Table 2.

It can be clearly seen from Table 2 that the AQ8-I and AQ8-II elements possess the same accuracy as that of the Q8 element when regular rectangular meshes are used. However, when distorted meshes are employed for analysis, the two new elements exhibit much superior stability than that of the Q8 element. Note that in this paper, all results of the Q8 element were obtained using the 3×3 Gauss integration rule. For this problem, the AQ8-I and AQ8-II elements produced almost the exact solution using different meshes.

The proposed area coordinate method is mainly for formulating straight-sided elements. However, the said elements developed can still work when one or more sides are curved (refer to the results of mesh 5 in Table 2). The procedure to make it work is simple, and it can be done by indicating the coordinates of the mid-side node of the curved side while keeping other things unchanged. It can

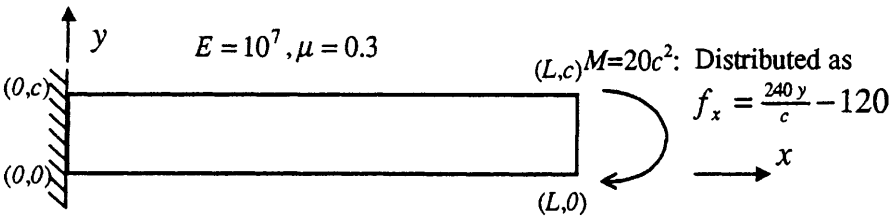

Fig. 5. Constant-bending-moment problem for cantilever

Table 2. Numerical results at selected locations for the constant-bending-moment problem

		Q8	Q12 [4]	AQ8-I	AQ8-II	Exact solution
Mesh 1	σ_x (0,10)	120.000	120.0	120.000	120.000	120.0
	σ_x (0,0)	−120.000	120.0	−120.000	−120.000	−120.0
	$v(100,0) \times 10^3$	−12.000	−12.00	−12.000	−12.000	−12.0
Mesh 2	σ_x (0,10)	56.447	125.5	118.222	118.222	120.0
	σ_x (0,0)	−74.863	−145.5	−114.667	−114.667	−120.0
	$v(100,0) \times 10^3$	−2.328	−5.18	−12.014	−12.014	−12.0
Mesh 3	σ_x (0+,10)	13.665	29.4	119.696	119.815	120.0
	σ_x (0,10−)	5.262	14.0	118.887	119.271	120.0
	σ_x (0,0+)	−5.665	−13.1	−119.112	−119.341	−120.0
	σ_x (0+,0)	−14.299	−28.5	−119.880	−119.866	−120.0
	$v(100,0) \times 10^3$	−0.477	−0.69	−11.997	−11.997	−12.0
Mesh 4	σ_x (0,10)	120.000	120.0	120.000	120.000	120.0
	σ_x (0,0)	−120.000	−120.0	−120.000	−120.000	−120.0
	$v(20,0) \times 10^4$	−4.8000	−4.800	−4.8000	−4.8000	−4.800
Mesh 5	σ_x (0,10)	120.244	–	124.977	124.977	120.0
	σ_x (0,0)	−120.244	–	−124.977	−124.977	−120.0
	$v(20,0) \times 10^4$	−4.689	–	−4.896	−4.896	−4.800

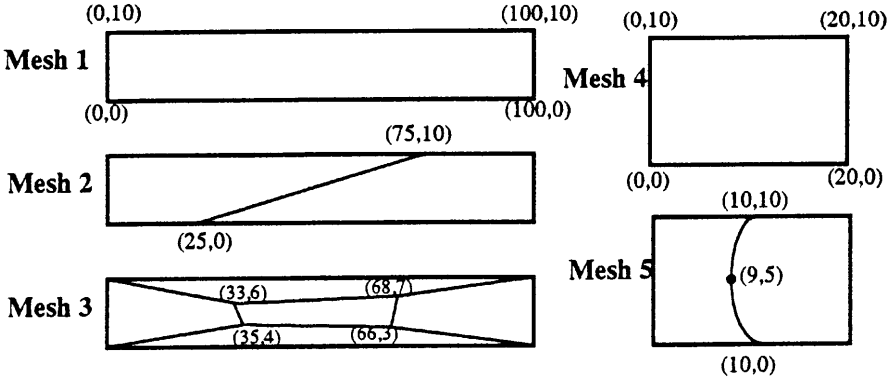

Fig. 6. Meshes devised for Example 2

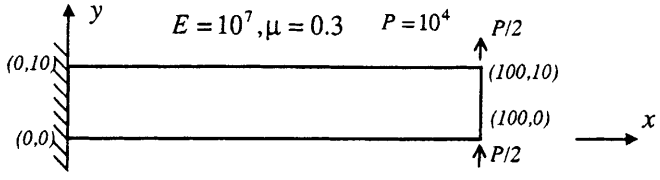

Fig. 7. Linear-bending problem for cantilever

Table 3. The deflection at a selected location for linear-bending problem of cantilever

		Q8	AQ8-I	AQ8-II	Exact solution
Mesh 1	v(100,0)	3.85	3.85	3.85	4.03
Mesh 2	v(100,0)	0.74	3.15	3.15	4.03
Mesh 3	v(100,0)	2.00	3.30	3.30	4.03
Mesh 4	v(100,0)	3.65	3.99	3.99	4.03

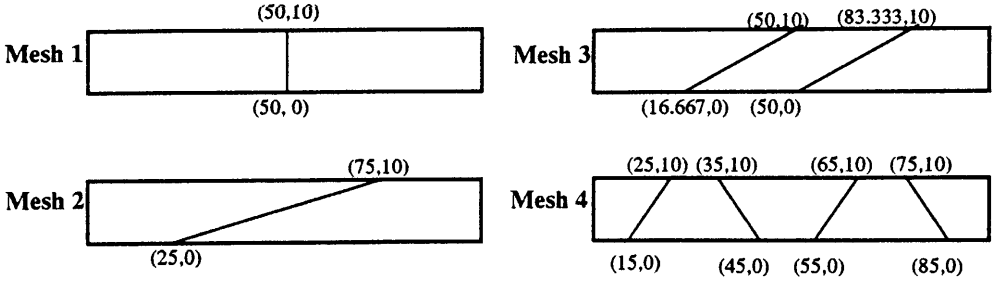

Fig. 8. Mesh for Example 3

be seen from Table 2 that the said elements are better than the Q8 element in terms of deflection. But the reverse is true for stresses.

Example 3. *Linear-bending problem for a cantilever beam* (refer to Fig. 7). The results of the deflection and stresses at selected points are shown in Table 3.

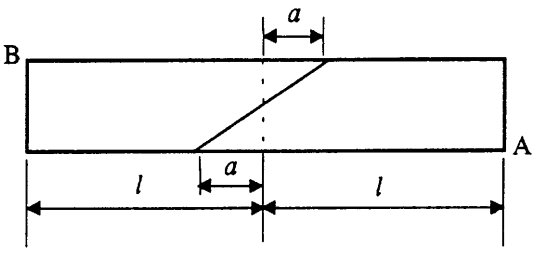

Fig. 9. Sensitivity test for mesh distortion

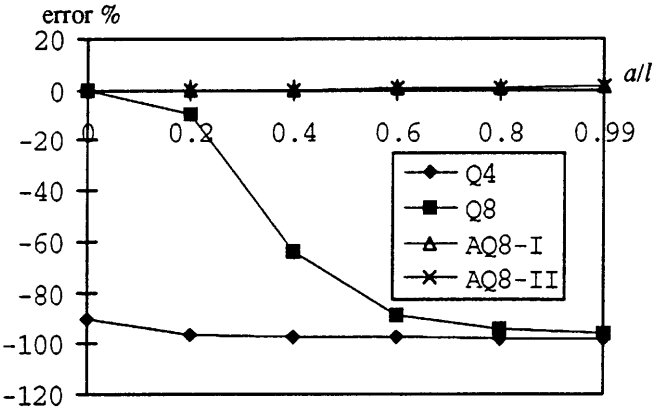

Fig. 10. Percentage error (%) of the deflection at point *A* in constant-bending problem due to mesh distortion

It is again obvious that the AQ8-I and AQ8-II elements perform better than the Q8 element when irregular meshes are used.

Example 4. *Sensitivity test for mesh distortion*. Re-perform examples 2 and 3 using the mesh shown in Fig. 9, where a varies from 0 to $0.99l$. The curves of the percentage errors are plotted in Figs. 10, 11 and 12.

From Figs. 10–12, it can be clearly seen that the two new elements are very insensitive to mesh distortion. For the quadratic problem (refer to Figs. 10 and 11), the AQ8-I and AQ8-II elements can almost produce the exact solution in the distorted conditions. For the cubic problem, their accuracy is also much higher than that of the Q8 element. This is to say the good performance of the proposed elements is not affected by mesh distortion. The above phenomena imply that the formulae for the displacement fields of the proposed elements have second order completeness in Cartesian coordinates. Thus, their performance is comparable to that of the Q9 Lagrangian element of straight-sides.

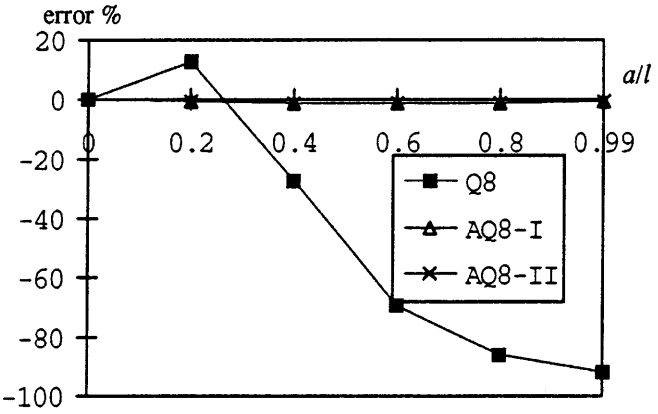

Fig. 11. Percentage error (%) of the sress σ_x at point *B* in constant-bending problem due to mesh distortion

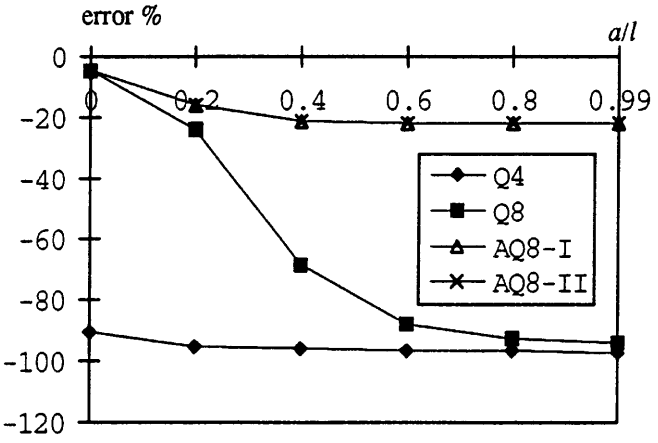

Fig. 12. Percentage error (%) of the deflection at point *A* in linear-bending problem due to mesh distortion

Example 5. *Cook's problem*. This example, in which a skew cantilever, as shown in Fig. 12, was subjected to a shear distributed load at the free edge, was proposed by Cook [10]. The results of the vertical deflection at point *C*, the maximum principal stress at point *A* and the minimum principal stress at point *B* are listed in Table 4.

Table 4. The results of Cook's problem

	V_c	$\sigma_{A(\max)}$	$\sigma_{B(\min)}$	V_c	$\sigma_{A(\max)}$	$\sigma_{B(\min)}$
	Mesh 1×1			Mesh 2×2		
Q8	17.22	0.1345	−0.1862	22.72	0.2472	−0.2261
AQ8-I	19.99	0.1559	−0.1928	22.98	0.2523	−0.2144
AQ8-II	19.99	0.1559	−0.1928	22.98	0.2523	−0.2144
	Mesh 4×4			Mesh 8×8		
Q8	23.71	0.2421	−0.2007	23.88	0.2390	−0.2041
AQ8-I	23.74	0.2415	−0.2024	23.89	0.2389	−0.2041
AQ8-II	23.74	0.2415	−0.2024	23.89	0.2389	−0.2041
Reference solution	23.95 [11]	0.2359 [12]	−0.2012 [12]	23.95 [11]	0.2359 [12]	−0.2012 [12]

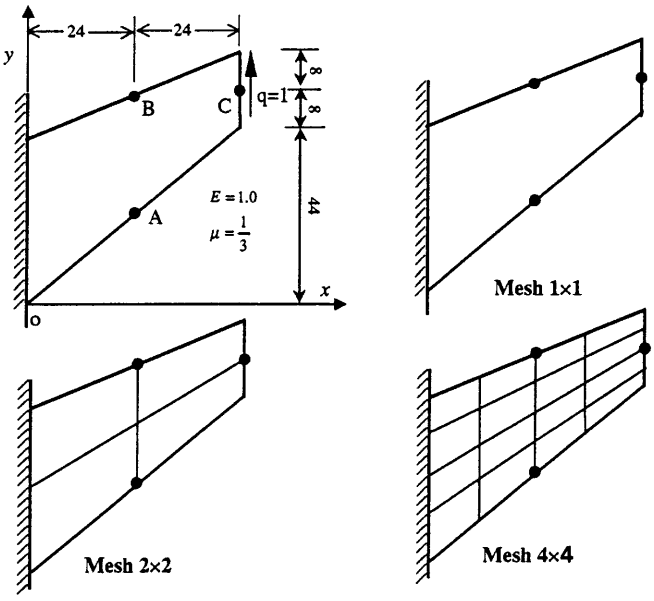

Fig. 13. Cook's problem

This example shows that the proposed elements converge faster than the Q8 element when irregular meshes are used.

6 Conclusions

Two eight-node quadrilateral membrane elements have been developed using area coordinates. The shape functions of these elements satisfy the generalized conforming conditions. The potential accuracy and versatility of the said elements have been illustrated using five numerical examples, which show that

1. The AQ8-I and AQ8-II elements have the same accuracy as the Q8 element when rectangular meshes are used.
2. For arbitrary quadrilateral meshes, the displacement fields of the proposed elements always possess second order completeness in Cartesian coordinates, which is not the case for the Q8 element. This is why the proposed elements are insensitive to mesh distortion but not the Q8 element. In fact, the performance of the proposed elements is comparable to that of the Q9 Lagrangian element of straight sides.
3. The two new elements can still work when the element sides are curved. It is worth noting that the results for displacement obtained by these two elements are still better than those of the Q8 element in some cases. However, it is recommended that a combination of the proposed and Q8 elements be used to study a practical problem in which curved meshing is required.

The work in this paper also demonstrate that the quadrilateral area coordinates method is an efficient tool for constructing simple, effective and reliable serendipity plane membrane elements.

Appendix: Evaluation of $\partial N_i/\partial x$ and $\partial N_i/\partial y$

The terms $\partial N_i/\partial x$ and $\partial N_i/\partial y$ can be expressed in the following manner suitable for computer coding:

Step 1:
For $i = 1$ to 4
$j = i + 1$ if $j > 4$ then $j = 1$
$k = j + 1$ if $k > 4$ then $k = 1$
$m = k + 1$ if $m > 4$ then $m = 1$

$$\frac{\partial N_i^0}{\partial L_i} = \frac{1}{2g_j}\left(1 - \frac{L_m}{g_i}\right) \quad \frac{\partial N_i^0}{\partial L_j} = \frac{1}{2g_m}\left(1 - \frac{L_k}{g_i}\right)$$
$$\frac{\partial N_i^0}{\partial L_k} = -\frac{L_j}{2g_m g_i} \quad \frac{\partial N_i^0}{\partial L_m} = -\frac{L_i}{2g_i g_j} \tag{A1}$$

For AQ8-I

$$\frac{\partial N_{4+i}}{\partial L_i} = \frac{2L_k}{g_i g_j}\left(1 + \frac{2L_j}{g_k + g_m} - \frac{2L_m}{g_i + g_j}\right)$$
$$\frac{\partial N_{4+i}}{\partial L_j} = \frac{4L_i L_k}{g_i g_j (g_k + g_m)}$$
$$\frac{\partial N_{4+i}}{\partial L_k} = \frac{2L_i}{g_i g_j}\left(1 + \frac{2L_j}{g_k + g_m} - \frac{2L_m}{g_i + g_j}\right) \tag{A2}$$
$$\frac{\partial N_{4+i}}{\partial L_m} = -\frac{4L_i L_k}{g_i g_j (g_i + g_j)}$$

For AQ8-II

$$\frac{\partial N_{4+i}}{\partial L_i} = \frac{4L_k}{g_i g_j}\left(L_j - L_m + \frac{g_i + g_j}{2}\right)$$
$$\frac{\partial N_{4+i}}{\partial L_j} = \frac{4L_i L_k}{g_i g_j}$$
$$\frac{\partial N_{4+i}}{\partial L_k} = \frac{4L_i}{g_i g_j}\left(L_j - L_m + \frac{g_i + g_j}{2}\right) \tag{A3}$$
$$\frac{\partial N_{4+i}}{\partial L_m} = -\frac{4L_i L_k}{g_i g_j}$$

End Step 1.
Step 2:
For $i = 1$ to 4
$j = i + 1$ if $j > 4$ then $j = 1$
$k = j + 1$ if $k > 4$ then $k = 1$
$m = k + 1$ if $m > 4$ then $m = 1$
For $ii = 1$ to 4

$$\frac{\partial N_i}{\partial L_{ii}} = \frac{\partial N_i^0}{\partial L_{ii}} - \left(\frac{1}{2} - \frac{g_i - g_j}{8g_m}\right)\frac{\partial N_{4+i}}{\partial L_{ii}} - \frac{g_k(g_j - g_k)}{8g_m g_i}\frac{\partial N_{4+j}}{\partial L_{ii}} + \frac{g_k(g_k - g_m)}{8g_i g_j}\frac{\partial N_{4+k}}{\partial L_{ii}} - \left(\frac{1}{2} + \frac{g_m - g_i}{8g_j}\right)\frac{\partial N_{4+m}}{\partial L_{ii}} \tag{A4}$$

End Step 2.
Step 3:
For $i = 1$ to 8

$$\frac{\partial N_i}{\partial x} = \frac{1}{2A}\left(b_1\frac{\partial N_i}{\partial L_1} + b_2\frac{\partial N_i}{\partial L_2} + b_3\frac{\partial N_i}{\partial L_3} + b_4\frac{\partial N_i}{\partial L_4}\right)$$
$$\frac{\partial N_i}{\partial y} = \frac{1}{2A}\left(c_1\frac{\partial N_i}{\partial L_1} + c_2\frac{\partial N_i}{\partial L_2} + c_3\frac{\partial N_i}{\partial L_3} + c_4\frac{\partial N_i}{\partial L_4}\right) \tag{A5}$$

End Step 3.

References

1. **Yuqiu Long, Juxuan Li, Zhifei Long, Song Cen** (1999) Area co-ordinates used in quadrilateral elements. Commun. Num. Meth. Eng. 15(8):533–545
2. **Zhifei Long, Juxuan Li, Song Cen, Yuqiu Long** (1999) Some basic formulae for area coordinates in quadrilateral elements. Commun. Num. Meth. Eng 15(12):841–852
3. **Stricklin JA, Ho WS, Richardson EQ, Haister WE** (1977) On isoparametric vs linear strain triangular elements. Int. J. Num. Meth. Eng. 11:1041–1043
4. **Lee NS, Bathe KJ** (1977) Effects of element distortions on the performance of isoparametric elements. Int. J. Num. Meth. Eng. 36:3553–3576
5. **Zienkiewicz OC, Taylor RL** (1989) The Finite Element Method. Fourth Edition, vol. 1. McGraw-Hill Book Company
6. **Long Yuqiu, Xin Kegui** (1989) Generalized conforming element for bending and bucking analysis of plates. Finite Elements in Analysis and Design 5:15–30
7. **Long Yuqiu, Bu Xiaoming, Xu Yin** (1995) Generalized conforming plate bending elements using point and line compatibility conditions. Comp. Struc. 54(4):717–723
8. **Shi Zhongci** (1990) On the accuracy of the quasi-conforming and generalized conforming finite elements. China Ann. Math. 11B(2):148–155
9. **Li JuXuan, Long Yuqiu** (1996) The convergence of the generalized conforming element method. Gong Cheng Li Xue/ Eng. Mech. 13(1):75–80 (in Chinese)
10. **Cook RD** (1986) On the Allman triangular and a related quadrilateral element. Comp. Struc. 22:1065–1067
11. **Felippa CA, Alexander S** (1992) Membrane triangular with corner drilling freedoms – III. Implementations and performance evolution. Finite Element Analysis in Design 12:203–249
12. **Bergan PG, Felippa CA** (1985) A triangular membrane element with rotational degrees of freedom. Comp. Meth. Appl. Mech. Eng. 50:25–69